

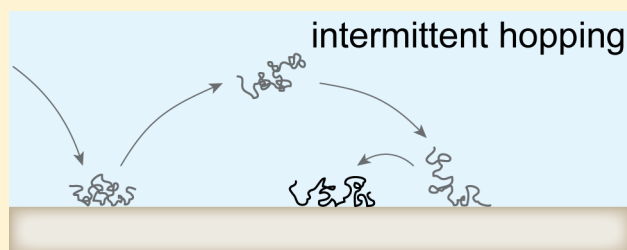
Single-Molecule Tracking of Polymer Surface Diffusion

Michael J. Skaug, Joshua N. Mabry, and Daniel K. Schwartz*

Department of Chemical and Biological Engineering, University of Colorado Boulder, Boulder, Colorado 80309, United States

S Supporting Information

ABSTRACT: The dynamics of polymers adsorbed to a solid surface are important in thin-film formation, adhesion phenomena, and biosensing applications, but they are still poorly understood. Here we present tracking data that follow the dynamics of isolated poly(ethylene glycol) chains adsorbed at a hydrophobic solid–liquid interface. We found that molecules moved on the surface via a continuous-time random walk mechanism, where periods of immobilization were punctuated by desorption-mediated jumps. The dependence of the surface mobility on molecular weight (2, 5, 10, 20, and 40 kg/mol were investigated) suggested that surface-adsorbed polymers maintained



effectively three-dimensional surface conformations. These results indicate that polymer surface diffusion, rather than occurring in the two dimensions of the interface, is dominated by a three-dimensional mechanism that leads to large surface displacements and significant bulk–surface coupling.

INTRODUCTION

In lubrication¹ and adhesion phenomena,² at biointerfaces, and in thin-film formation processes,³ polymer molecules adsorb to a solid surface,⁴ and their dynamics govern subsequent relaxation and transport. While the motion of polymers in the “melted” state or in solution is fairly well understood,⁵ the mechanisms by which polymers move on surfaces remain mysterious and a matter of debate.^{6–12} It is clear, however, that polymer dynamics are significantly slowed near an attractive interface.^{4,13} For example, surface diffusion coefficients are often orders of magnitude lower than bulk values,^{4,14} but the available experimental evidence does not conclusively identify a dominant mechanism of polymer surface diffusion and suggests that the mechanism may depend on the surface and the chain length.^{9,10}

Part of the difficulty in understanding polymer surface dynamics is that polymer surface conformations may be different than bulk conformations and can vary depending on the polymer–surface interaction, the chain length, and surface coverage.¹³ The conventional picture is that polymers adsorb to a solid surface with a “loop–train–tail” conformation in which adsorbed chain segments are “trains” separated by “loops” of unadsorbed monomers.¹³ The bound fraction (the fraction of polymer segments adsorbed in trains) is one measure of the adsorbed chain conformation. The equilibrium bound fraction is predicted to depend on the monomer–surface interaction energy, χ_s , and the chain length, N . For short chains ($N < 10$) or strongly adsorbing monomers ($\chi_s > 1kT$), the bound fraction approaches unity, while for longer chains or weakly attractive monomers, the bound fraction is typically in the range 0.5 to 1.^{6,15} Previous experiments have found bound fractions between 0.5 and 0.75 for polymers adsorbed at low surface coverage, suggesting a flattened two-dimensional conformation.^{9,16} However, this picture is further complicated if adsorbed chains relax toward equilibrium very slowly.^{17,18} Whether an adsorbed chain is strictly two-dimensional or in a more three-dimensional

conformation has a significant influence on the possible mechanism by which a polymer moves across a surface.

To uncover the detailed mechanism of polymer surface diffusion, we conducted a series of single-molecule tracking experiments to probe the behavior of isolated linear homopolymer chains at a hydrophobic solid–aqueous interface. Specifically, we studied a series of poly(ethylene glycol) (PEG) chains whose molecular weight varied by more than an order of magnitude. The primary driving force for PEG adsorption to the solid surface was the hydrophobic interaction.^{9,19} Because the hydrophobic interaction is nonspecific and relatively long-ranged compared with other intermolecular forces, the system we studied represents the case of a delocalized, long-range polymer–surface interaction.

We observed polymer surface transport characterized by desorption-mediated displacements that were interrupted by periods of immobility, qualitatively similar to a previous report for the surface diffusion of other molecular species.²⁰ A desorption-mediated surface displacement is one where, instead of moving in the plane of the surface, the molecule desorbs, diffuses in the bulk liquid, and readsorbs at a new surface location. A specific example of a continuous-time random walk,²¹ this mechanism can be described as “intermittent hopping” because each desorption-mediated surface displacement is separated by a random period of apparent surface immobilization. One consequence of the desorption-mediated mechanism is that large displacements are much more probable than if the process involved normal (Gaussian) Brownian motion within the plane of the surface. The prevalence of large surface displacements and the intermittency of the trajectories are predicted to dramatically influence the rate at which a polymer finds a surface target,^{22,23} a key process in heterogeneous catalysis, biosensing, and other

Received: July 18, 2013

Published: November 10, 2013

technologies. Our results also highlight the fact that surface diffusion is not necessarily a two-dimensional process but is coupled to three-dimensional motion near the surface, potentially making surface diffusion sensitive to the near-surface liquid environment. In fact, our observations imply strong bulk–surface coupling, where the average diffusion of polymers well away from the surface is reduced.¹⁴

EXPERIMENTAL SECTION

Single-Molecule Tracking. We used total internal reflection fluorescence microscopy (TIRFM)²⁰ to track the motion of individual polymer chains at a planar interface between aqueous solution and polished fused silica coated with a hydrophobic trimethylsilyl (TMS) monolayer.²⁴ We collected image sequences of fluorescently labeled polymers as they randomly adsorbed and moved on the surface at dilute surface coverage. Using custom image analysis in Mathematica, we identified the positions of the polymers in each image and extracted molecular surface trajectories from the image sequences (Figure 1a). The polymer chains were PEG of nominal molecular weights 2, 5, 10, 20, and 40 kg/mol, corresponding to $N = 45, 113, 227, 454,$ and 908 monomer units. The polymer was end-labeled with fluorescein isothiocyanate (PEG, Nanocs, USA). The PEG samples were dissolved at low concentration (10 fM to 600 pM) in 1 mM sodium borate buffer at pH 8.6 and injected into a custom flow cell and imaged as previously described.²⁴ In a control experiment, we found that fluorescein isothiocyanate does not adsorb appreciably to the surface at the concentrations used in this study, indicating that the PEG–surface interaction was the dominant driving force for polymer surface adsorption. We estimate that the PEG monomer–surface interaction energy in our experiments was similar to the value of $\sim 0.5kT$ measured on a similar hydrophobic surface.⁹ The bulk concentrations were selected such that the surface coverage was approximately 0.01 molecule/ μm^2 ($\sim 10^{-3}$ mg/ m^2), meaning that the measurements were made in the dilute limit where no polymer–polymer interactions were expected. Although the degree of labeling was not verified, a small amount of unlabeled polymer would not be expected to influence the dynamics at such dilute concentrations. Image sequences of polymer adsorption, diffusion, and desorption were recorded with an exposure time of 0.05 or 0.1 s. Because of their fast diffusion ($D > 10 \mu\text{m}^2/\text{s}$) in solution, molecules could be identified and tracked only when they were adsorbed to the solid surface. Trajectories were constructed by connecting nearest-neighbor objects in consecutive frames given a maximum allowed displacement of $R_{\text{max}} = 2.2 \mu\text{m}$. The possibility of falsely connecting two molecules into a single trajectory was recently discussed,²⁰ and all of the results are based on trajectories that lasted more than 2 s.

Simulations. To simulate molecular surface trajectories, we used a model similar to one that was previously described,²⁰ except that the desorption-mediated surface displacements were drawn from the recently published exact expression for $W(r)$, the distribution of individual surface displacements produced by excursions through the bulk liquid:²⁵

$$W(r) = \frac{1}{2\pi r(r^*)} - \frac{1}{4(r^*)^2} \left[H_0\left(\frac{r}{r^*}\right) - Y_0\left(\frac{r}{r^*}\right) \right] \quad (1)$$

where H_0 is the Struve function, Y_0 is a Bessel function of the second kind, and the parameter $r^* = D/(Q_{\text{ads}}b)$ incorporates the fundamental physical parameters of the system: the bulk diffusion coefficient D , the adsorption rate constant Q_{ads} , and the polymer radius of gyration b . Equation 1 is valid at time scales longer than a typical desorption-mediated displacement, which was the case in our experiments where displacements were effectively instantaneous. The empirical waiting-time distributions $\psi(\tau_{\text{des}})$ were modeled using the expression

$$\psi(\tau_{\text{des}}) = \left[\frac{\alpha^{1-\alpha}}{\langle \tau_{\text{des}} \rangle^{-\alpha} (\alpha - 1)^{-\alpha}} \right] \left(\frac{1}{\tau_{\text{des}}} \right)^{1+\alpha}$$

where $\alpha = 1.5$ and the mean waiting time $\langle \tau_{\text{des}} \rangle$ were measured experimentally.²⁰ During each period of immobilization, random spatial

fluctuations, taken from the distribution $f_{\text{vib}}(r) = [l(2\pi)^{1/2}]^{-1} \exp(-r^2/2l^2)$ with $l = 0.04 \mu\text{m}$, were added to the molecular position to account for apparent motion due to experimental localization uncertainty. After each random waiting time, a random surface displacement was selected using eq 1. The constant $r^* = D/(Q_{\text{ads}}b)$ contains three parameters, but the bulk diffusion coefficient D and the radius of gyration b can be set to known or independently calculated values, leaving Q_{ads} as the only free parameter used in the simulations to match the experimental results. The complete set of simulation parameters are provided in Table S1 in the Supporting Information. The diffusion coefficients were taken from the literature,²⁶ and the radius of gyration was calculated using $b = aN^{3/5}$, where $a = 0.35 \text{ nm}$ is the PEG monomer size.²⁷

RESULTS

In analyzing the motion of individual polymer chains as they moved at the interface between a buffer solution and a hydrophobic substrate, a notable qualitative observation involved the significant heterogeneity between molecular trajectories (Figure 1b).

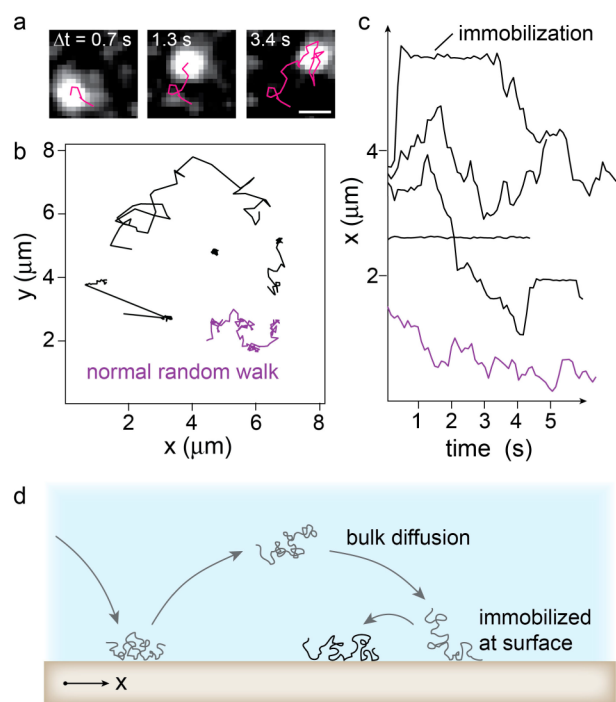


Figure 1. Intermittent-hopping mechanism of polymer surface diffusion. (a) Experimental fluorescence images of a 40 kg/mol PEG polymer moving at the solid–liquid interface. The scale bar represents 1.0 μm . (b) Representative trajectories of 40 kg/mol polymers that illustrate the intermittent nature of the dynamics. For comparison, a normal random walk (generated via a computer simulation) with the same effective diffusion coefficient as the experimental trajectories is depicted in magenta. (c) Data for the 40 kg/mol polymer showing lateral position as a function of time to highlight the periods of immobility. (d) Illustration of the proposed desorption-mediated mechanism governing polymer surface diffusion.

Some trajectories appeared to be completely immobile while others were mobile or displayed intermittent behavior. We also noted the occurrence of some very large displacements across the surface (Figure 1b). These two observations are qualitatively inconsistent with the behavior expected for a molecule diffusing via normal Brownian motion in two dimensions. The same qualitative behavior was observed for all of the molecular weights studied and was similar to the dynamics reported for the surface diffusion of other molecular species.^{20,28}

To quantify the polymer surface dynamics, we analyzed the distributions of molecular surface displacements (Figure 2) using the self-part of the van Hove correlation function,

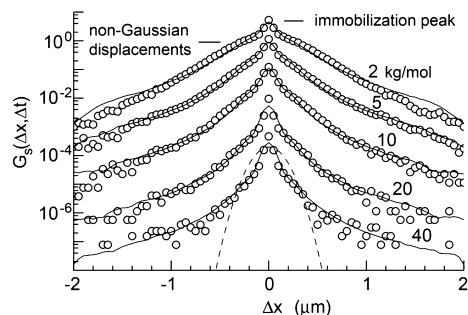


Figure 2. Distributions of surface displacements. The symbols represent experimental data for PEG of different molecular weights (as annotated) at the solid–liquid interface for a time interval $\Delta t = 0.1$ s. The solid lines are simulation results using the model described in the text. The dashed line is a Gaussian with the same effective diffusion coefficient as the 40 kg/mol data ($D \approx 0.075 \mu\text{m}^2/\text{s}$). The curves were shifted vertically to allow easier interpretation (the 2, 5, 10, 20, and 40 kg/mol data sets were shifted by factors of 3, 5, 0.5, 0.02, and 0.001, respectively).

$$G_s(\Delta x, \Delta t) = \frac{1}{N} \left\langle \sum_{i=1}^N \delta[\Delta x + x_i(t) - x_i(t + \Delta t)] \right\rangle \quad (2)$$

This distribution represents the probability that a molecule has moved a distance Δx along the x or y coordinate during time Δt . The two salient qualitative features of the measured displacement distributions are the narrow central peaks and the non-Gaussian tails (Figure 2). The tails of the distributions evolve from approximately exponential for the polymer with the lowest molecular weight to approximately power-law for the largest polymer (the non-Gaussian tails of the distributions are highlighted in Figure S1 in the Supporting Information). This contrasts with the Gaussian distribution that would be expected if the polymer chains were undergoing normal two-dimensional Brownian motion at the interface. Qualitatively, we observed the expected decrease in mobility with increasing molecular weight, as evidenced by the narrowing of the displacement distributions (Figure 2). However, as illustrated by the dashed line in Figure 2, a simple random-walk model for surface diffusion certainly does not describe the central peaks and non-Gaussian tails of the distributions.

The narrow central peaks of the displacement distributions do not broaden with increasing lag time (Figure S2 in the Supporting Information), suggesting that they are associated with periods of immobility or confinement.²⁰ We believe that the finite width of the central peaks is primarily due to imperfect localization of molecules in the fluorescence images.²⁹ In fact, the width of the central peaks, $\sigma \approx 0.04 \mu\text{m}$, is a measure of our experimental localization precision and implies that we were able to resolve only displacements much greater than the polymer coil size. Although there may have been confined or slow diffusion ($D < 0.002 \mu\text{m}^2/\text{s}$) during periods of apparent immobility, the molecules appeared immobilized given our experimental localization precision and trajectory lengths.

The intermittency of the trajectories can be characterized statistically by the distribution of waiting times, τ_{des} , between surface displacements. Using the displacement distributions as a

guide, we defined a distance threshold of $\Delta r = 0.2 \mu\text{m}$ to distinguish real surface displacements from apparent motion during immobilization. For all polymer chain lengths, we found that the periods of immobilization were characterized by the same approximately power-law distribution of waiting times, $\psi(\tau_{\text{des}}) \sim \tau_{\text{des}}^{-(1+\alpha)}$, where $\alpha = 1.5$ (Figure 3). As one would

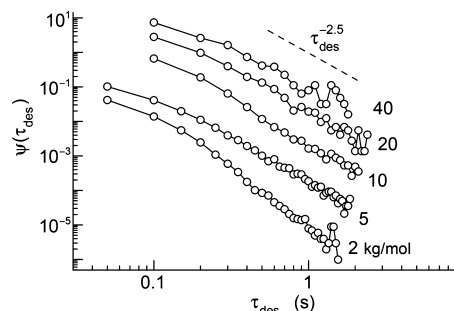


Figure 3. Distributions of the waiting time between desorption-mediated surface displacements. Symbols with connecting lines are the experimental data for PEG of different molecular weight (as annotated). Curves were displaced vertically to allow easier interpretation (the 2, 5, 20, and 40 kg/mol data sets were shifted by factors of $1/15$, $1/5$, 5, and 15, respectively.) The dashed line illustrates the approximate $\tau_{\text{des}}^{-2.5}$ behavior of the distributions.

intuitively expect, we found that the mean waiting time, $\langle \tau_{\text{des}} \rangle$, increased with increasing chain length. A theoretical prediction for this increase, based on equilibrium configurations of adsorbed chains, is that the mean desorption time should scale as e^N , where N is the number of monomers.³⁰ However, we observed power-law scaling of the mean desorption time: $\langle \tau_{\text{des}} \rangle \sim N^\beta$, where $\beta = 0.6 \pm 0.1$ (Figure 4a). The significance of this exponent is discussed in more detail below. This finding was robust with respect to variations in the data analysis parameters. For example, changing the distance threshold used to define immobilization by $\pm 0.04 \mu\text{m}$ resulted in a $\pm 18\%$ change in mean waiting time and little change in the approximate power-law exponent.

Despite the non-Gaussian displacement distributions, we found that the mean-square displacement (MSD) increased approximately linearly with time (Figure 5). In the absence of the displacement distributions (Figure 2), this would be consistent with normal Brownian motion, that is, the MSD is insensitive to the detailed mechanism of surface diffusion, as has been previously observed.^{20,31} The roughly equal spacing between the MSD curves in Figure 5 suggests a power-law dependence of the transport coefficient on chain length. To characterize this dependence in a way that allows comparison with previous reports, we calculated an *effective* surface diffusion coefficient at short times, D_{eff} by fitting the MSD to a linear model over the first four data points. We found that $D_{\text{eff}} \sim N^\gamma$, where $\gamma = -0.6 \pm 0.2$ (Figure 4b).

As mentioned above, the non-Gaussian tails of the displacement distributions (Figure 2) are not consistent with a normal two-dimensional random walk. Interestingly, power-law-distributed displacements were predicted theoretically for interfacial molecular motion dominated by desorption-mediated diffusion.³² Desorption-mediated surface displacements occur when a molecule desorbs from the interface, begins diffusing in the adjacent three-dimensional bulk (liquid) phase, and readsorbs at a new location on the surface before being lost completely from the surface.^{25,32} In the standard model, this occurs under strongly adsorbing conditions defined by the molecule's surface

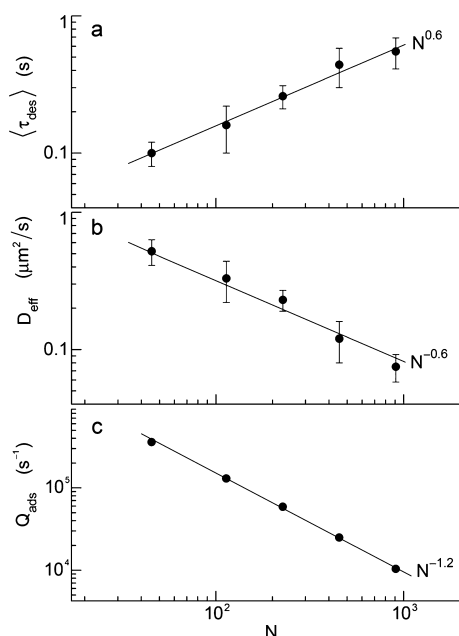


Figure 4. Chain length scaling of polymer surface dynamics and kinetics. (a, b) Plots of (a) the mean waiting time and (b) the effective surface diffusion coefficient vs the chain length N (i.e., the degree of polymerization). Symbols are experimental data, and the solid lines depict the scalings $\langle \tau_{\text{des}} \rangle \sim N^\beta$ and $D_{\text{eff}} \sim N^\gamma$, where the best-fit exponents are $\beta = 0.6 \pm 0.1$ and $\gamma = -0.6 \pm 0.2$, respectively. The error bars are standard deviations from five random subsets of the data. (c) Scaling of the adsorption rate with chain length, as determined by fitting the experimental displacement distributions with the model for intermittent hopping. The solid line depicts the scaling $Q_{\text{ads}} \sim N^\delta$, where $\delta = -1.2 \pm 0.1$.

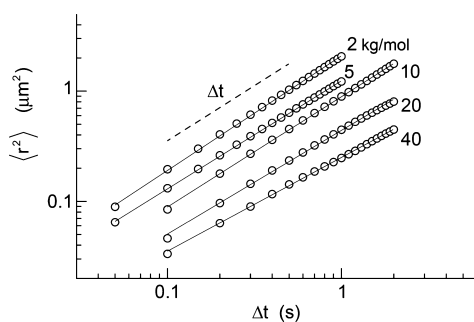


Figure 5. Mean square displacement as a function of time. Symbols are experimental data for PEG of different molecular weights (as annotated), and solid lines are least-squares fits to the expression $\langle r^2 \rangle = 4\Gamma(\Delta t)^\alpha$. The best-fit exponents are $\alpha = 1.04(1)$, $0.98(3)$, $1.00(5)$, $0.94(8)$, and $0.9(1)$ for the 2, 5, 10, 20, and 40 kg/mol data, respectively. The dashed line illustrates the linear dependence of the MSD on time (i.e., Fickian diffusion).

interaction and bulk diffusivity.³³ Strong adsorption implies that the molecule desorbs and reabsorbs many times before it is finally lost to the bulk. The resulting desorption-mediated steps are power-law-distributed, and the many-step displacement distribution is a Cauchy distribution with power-law tails.²⁵ It should also be noted that the predicted Cauchy distribution holds only over limited time and length scales and transforms into a Gaussian distribution at long times and lengths.²⁵

To compare our experimental results with the standard model for desorption-mediated displacements, in principle one could attempt to fit the tails of the displacement distributions in

Figure 2 with the predicted Cauchy distribution.^{25,32} However, the standard theoretical model assumes a single desorption time, which is inconsistent with the experimentally measured waiting-time distributions (Figure 3), which exhibited long tails. We therefore chose to simulate the molecular surface trajectories using the empirical waiting-time distributions (Figure 3) and the analytical expression for the distribution of single-desorption-mediated displacements $W(r)$ (eq 1). Using Q_{ads} (the adsorption rate constant) as the only free parameter in the simulations, we found reasonable agreement with the experimental displacement distributions (Figure 2) when Q_{ads} decreased with increasing molecular weight (Figure 4c). In fact, we found the approximate scaling $Q_{\text{ads}} \sim N^\delta$, where $\delta = -1.2 \pm 0.1$.

We note that the standard model for desorption-mediated diffusion, which assumes a single characteristic desorption time, predicts superdiffusive behavior in strongly adsorbing systems,^{25,32} yet the measured MSD was either Fickian or slightly subdiffusive (Figure 5). The most likely reason for this discrepancy is the existence of long periods of immobilization over the entire experimental time scale (Figure 1c), as opposed to a single characteristic desorption time.^{25,32}

DISCUSSION

Dependence of the Chain Dynamics on Molecular Weight. We observed polymer surface diffusion that was well-described by an intermittent-hopping mechanism. Moreover, the chain dynamics exhibited a clear and systematic dependence on the molecular weight. On the basis of statistical models of polymer chain conformations, it is possible to interpret this chain-length dependence to obtain additional information about polymer conformations and dynamics. In what follows, we examine the implications of the observed dynamic scaling and how it compares with previous ideas about polymer surface behavior.

We start with the scaling of Q_{ads} , which can be rationalized in terms of p , the probability that the chain adsorbs during each surface encounter. The adsorption rate is $Q_{\text{ads}} = p/\tau_{\text{coil}}$ where $\tau_{\text{coil}} = b^2/D$ is the time that the polymer chain remains within a distance b of the surface (i.e., in contact with the surface) if it has a bulk diffusion coefficient D . With the assumption that each monomer–surface interaction is identical, $p \sim N^\nu$ follows from the fact that the number of monomers in contact with the surface scales as N^ν .^{9,13} Because $b \sim N^\nu$ and $D \sim N^{-\nu}$ for a polymer in dilute solution,⁵ it follows that $Q_{\text{ads}} \sim N^{-2\nu}$. Assuming good solvent conditions for PEG in water (i.e., $\nu = 0.6$) leads to the prediction that $Q_{\text{ads}} \sim N^{-1.2}$, as observed.

The scaling discussed above also leads to a surprising prediction for equilibrium polymer adsorption, which was identified in earlier experiments.⁹ In adsorption isotherm measurements, the adsorption rate and desorption rate (or inverse mean waiting time $\langle \tau_{\text{des}} \rangle^{-1}$) combine to give the slope of the isotherm, $h = Q_{\text{ads}}b/\langle \tau_{\text{des}} \rangle^{-1}$. Using our previously outlined scaling theory for Q_{ads} and b and noting our empirical finding for the scaling of $\langle \tau_{\text{des}} \rangle^{-1}$, we infer that h would be independent of the polymer molecular weight. This extrapolation from our single-molecule results is consistent with macroscopic adsorption measurements made on a similar experimental system consisting of PEG at a hydrophobic–water interface.⁹

Interestingly, these observations suggest that the difference between the diffusive behaviors of short and long chains is primarily due to the times of immobilization and not the step sizes during mobile periods. To see this, we note that the surface is modeled as an adsorptive sink of width b with strength

proportional to Q_{ads} . For comparison, a perfectly adsorbing sink of the same strength would have a width $r^* = D/(Q_{\text{ads}}b)$. On the basis of our above scaling arguments, r^* does not have an explicit dependence on molecular weight, suggesting that the time-independent step size distribution $W(r)$ (eq 1) is also independent of molecular weight. Thus, the differences between the displacement distributions shown in Figure 2 are governed by differences in the waiting-time distributions.

The invariance of the step-size distribution $W(r)$ with molecular weight is also consistent with the observed scaling of the effective surface diffusion coefficient, D_{eff} . If $D_{\text{eff}} \sim \langle W(r)^2 \rangle / \langle \tau_{\text{des}} \rangle$ and $W(r)$ is constant, then D_{eff} would be expected to scale as the desorption rate $\langle \tau_{\text{des}} \rangle^{-1}$; this is precisely what we found by fitting the data in Figure 4 (i.e., $D_{\text{eff}} \sim \langle \tau_{\text{des}} \rangle^{-1} \sim N^{-0.6}$).

This scaling of the surface diffusion coefficient with chain length differs from what was found in previous investigations. Conventional theory and simulations of polymer surface diffusion (which assume a two-dimensional model for displacements) predict that the surface diffusion coefficient should scale as $D \sim N^{-\alpha}$ with exponents in the range $3/4 < \alpha < 3/2$,^{6–9} but those models do not consider desorption as a mechanism of polymer surface transport. Previous experimental measurements of polymer surface dynamics using fluorescence correlation spectroscopy (FCS) found that the apparent diffusion coefficient scaled as $N^{-3/2}$ or N^{-1} .^{9,10} The difference between the scaling exponents in our observations and previous FCS experiments suggests either that there was a fundamentally different transport mechanism or that the experimental methods were sensitive to different features of the dynamics. FCS measures temporal fluctuations, so it cannot explicitly distinguish between intensity fluctuations that arise from adsorption/desorption events and lateral diffusion through a defined focal volume. In the current model, surface diffusion and desorption occur via the same temporal process, and our observed distribution of waiting times $\psi(\tau_{\text{des}}) \sim \tau_{\text{des}}^{-(1+\alpha)}$ with $\alpha = 1.5$ would contribute a decay of $\sim \tau^{-1.5}$ to the fluorescence correlation, similar to the $\sim \tau^{-1.0}$ decay assumed for Gaussian diffusion in an FCS experiment. We also cannot rule out the possibility that subtle differences in the experimental systems used (e.g., long-chain alkane surfaces in which chains might become entangled vs our TMS surfaces) may also result in fundamentally different polymer dynamics.

In contrast to earlier work that found different chain-length-dependent dynamic regimes,¹⁰ we found that a single desorption-mediated mechanism explains all of our experimental data. Over the range of molecular weights studied, there was no apparent transition in the dynamics, for example, from a desorption-mediated mechanism for small chains to an in-plane mechanism for longer chains. Although it is possible that our limited localization precision masked a very slow, in-plane diffusive mode ($< 0.002 \mu\text{m}^2/\text{s}$), the experimental data showed only intermittent immobilization and desorption-mediated displacements.

Implications of a Power-Law Waiting-Time Distribution. A typical intuitive model for intermittent immobilization involving a single characteristic surface-binding energy would predict a decaying exponential distribution of waiting times. However, the measured waiting-time distributions observed here were systematically broader than an exponential; all followed the approximate scaling $\psi(\tau_{\text{des}}) \sim \tau_{\text{des}}^{-(1+\alpha)}$ with $\alpha = 1.5$ (Figure 3). The same universal scaling was observed previously²⁰ and suggests that polymer desorption from the interface was characterized by a spectrum of binding energies; power-law relaxation naturally arises when there is a mixture of exponential

processes.^{34,35} A spectrum of binding energies might result from polymer chains having long-lived, nonequilibrium binding configurations or from chains having a distribution of adsorbed “train” lengths.^{17,36} A power-law distribution of waiting times was also observed for DNA-coated particles moving on a surface, where the number of particle–surface bonds was a random quantity.³⁵

There are two possible interpretations of the power-law scaling of the mean waiting time (Figure 4a). If all of the adsorbed segments were released at the same time, there would be a single energy barrier to desorption, and the waiting time would have an exponential dependence on the barrier height.^{37,38} Our simulations suggested that the polymer adsorbed from solution with $\sim N^{0.6}$ monomers in contact with the surface. If desorption occurred from the same conformation (i.e., if relaxation of the chain on the surface was slow), the desorption energy would have scaled as $\sim N^{0.6}$, giving rise to a stretched exponential increase in mean waiting time (which might appear similar to a power law over a limited measurement range). The second possibility is that bound segments of the polymer chains desorbed in a step-by-step rather than a concerted manner. When adsorbed chain segments detach sequentially and are kinetically independent of each other, the time for chain detachment has a power-law dependence on the chain length.³⁸ We favor the second interpretation because a desorption mechanism involving sequential, kinetically independent events is also consistent with the power-law waiting-time distributions discussed above.

Three-Dimensional Surface Conformations. The scaling exponents we observed (0.6, -0.6 , and -1.2) are reminiscent of the so-called Flory exponent for a three-dimensional chain in a good solvent ($\nu = 0.6$); for example, the characteristic size (radius of gyration) of a three-dimensional coiled chain exhibits this same dependence on molecular weight. This suggests that the PEG chains in these experiments, even when in contact with the hydrophobic surface, adopted conformations similar to those expected in bulk solution. In contrast, if the adsorbed chains adopted strictly two-dimensional conformations (pancakes), the number of adsorbed monomers would increase in proportion to N , and the waiting times would fall off exponentially with chain length rather than as a power law as we observed. That we should find behavior appropriate for a three-dimensional chain contrasts with conventional equilibrium models and many experiments that find a flattened, two-dimensional conformation for adsorbed polymers.^{9,39,40} More extended three-dimensional conformations might be the result of weak adsorption or a very slow approach to equilibrium that prevented the chains from flattening onto the surface before they desorbed back into solution.

CONCLUSIONS

We observed polymer surface diffusion that was dominated by a desorption-mediated mechanism, where chains desorb from the interface, diffuse in the bulk liquid, and re-adsorb at a new surface location. Systematically varying the polymer–surface interaction, or the topographic and chemical heterogeneity of the surface, would help test the universality of the intermittent-hopping mechanism. For example, an in-plane diffusion mechanism could become dominant in systems with larger molecular weight, stronger surface interaction, or smaller in-plane energy barriers. However, in the system studied here, and for a variety of other molecules,²⁰ desorption-mediated diffusion dominated. As a consequence, although polymers are essentially immobilized when in contact with the surface, large surface displacements are

still possible. In fact, large displacements are more probable than if polymer chains diffused in the plane of the surface. Intermittent hopping also implies a stronger surface–bulk coupling than is commonly assumed and could help explain the previously observed long-range effect of an attractive surface on polymer diffusion and the nonexponential decay of surface coverage.^{14,30} Additional insight into polymer surface dynamics could also be provided by methods that directly probe molecular conformation, as our results suggest but do not prove the existence of three-dimensional nonequilibrium surface-bound polymer conformations.

■ ASSOCIATED CONTENT

● Supporting Information

Figures S1 and S2 and Table S1 containing simulation parameters. This material is available free of charge via the Internet at <http://pubs.acs.org>.

■ AUTHOR INFORMATION

Corresponding Author

daniel.schwartz@colorado.edu

Notes

The authors declare no competing financial interest.

■ ACKNOWLEDGMENTS

The authors acknowledge support from the U.S. Department of Energy, Office of Basic Energy Sciences, Chemical Sciences, Geosciences, and Biosciences Division (DE-SC0001854). We also acknowledge Dr. Robert Walder for his critical reading of the manuscript.

■ REFERENCES

- (1) Urbakh, M.; Klafter, J.; Gourdon, D.; Israelachvili, J. *Nature* **2004**, *430*, 525.
- (2) Müller, C.; Müller, A.; Pompe, T. *Soft Matter* **2013**, *9*, 6207.
- (3) Schwartz, D. K. *Annu. Rev. Phys. Chem.* **2001**, *52*, 107.
- (4) Granick, S.; Kumar, S. K.; Amis, E. J.; Antonietti, M.; Balazs, A. C.; Chakraborty, A. K.; Grest, G. S.; Hawker, C.; Janmey, P.; Kramer, E. J. *J. Polym. Sci., Part B: Polym. Phys.* **2003**, *41*, 2755.
- (5) Rubinstein, M.; Colby, R. *Polymer Physics*; Oxford University Press: New York, 2003.
- (6) Milchev, A.; Binder, K. *Macromolecules* **1996**, *29*, 343.
- (7) Desai, T. G.; Keblinski, P.; Kumar, S. K.; Granick, S. *Phys. Rev. Lett.* **2007**, *98*, No. 218301.
- (8) Mukherji, D.; Bartels, G.; Müser, M. H. *Phys. Rev. Lett.* **2008**, *100*, No. 068301.
- (9) Sukhishvili, S. A.; Chen, Y.; Müller, J. D.; Gratton, E.; Schweizer, K. S.; Granick, S. *Macromolecules* **2002**, *35*, 1776.
- (10) Wong, J. S. S.; Hong, L.; Bae, S. C.; Granick, S. *Macromolecules* **2011**, *44*, 3073.
- (11) Maier, B.; Rädler, J. O. *Phys. Rev. Lett.* **1999**, *82*, 1911.
- (12) Granick, S.; Bae, S. C. *J. Polym. Sci., Part B: Polym. Phys.* **2006**, *44*, 3434.
- (13) Fleer, G. J.; Cohen Stuart, M. A.; Scheutjens, J. M. H. M.; Cosgrove, T.; Vincent, B. *Polymers at Interfaces*; Chapman and Hall: London, 1993.
- (14) Zheng, X.; Rafailovich, M.; Sokolov, J.; Strzhemechny, Y.; Schwarz, S.; Sauer, B.; Rubinstein, M. *Phys. Rev. Lett.* **1997**, *79*, 241.
- (15) Lai, P.-Y. *Phys. Rev. E* **1994**, *49*, 5420.
- (16) Douglas, J. F.; Schneider, H. M.; Frantz, P.; Lipman, R.; Granick, S. *J. Phys.: Condens. Matter* **1997**, *9*, 7699.
- (17) O'Shaughnessy, B.; Vavylonis, D. *J. Phys.: Condens. Matter* **2005**, *17*, R63.
- (18) Chakraborty, A. K.; Adriani, P. M. *Macromolecules* **1992**, *25*, 2470.
- (19) Meyer, E. E.; Rosenberg, K. J.; Israelachvili, J. *Proc. Natl. Acad. Sci. U.S.A.* **2006**, *103*, 15739.
- (20) Skaug, M. J.; Mabry, J. N.; Schwartz, D. K. *Phys. Rev. Lett.* **2013**, *110*, No. 256101.
- (21) Klafter, J.; Sokolov, I. M. *First Steps in Random Walks: From Tools to Applications*; Oxford University Press: New York, 2011.
- (22) Benichou, O.; Loverdo, C.; Moreau, M.; Voituriez, R. *Phys. Chem. Chem. Phys.* **2008**, *10*, 7059.
- (23) Lomholt, M. A.; Tal, K.; Metzler, R.; Joseph, K. *Proc. Natl. Acad. Sci. U.S.A.* **2008**, *105*, 11055.
- (24) Skaug, M. J.; Schwartz, D. K. *Soft Matter* **2012**, *8*, 12017.
- (25) Chechkin, A. V.; Zaid, I. M.; Lomholt, M. A.; Sokolov, I. M.; Metzler, R. *Phys. Rev. E* **2012**, *86*, No. 041101.
- (26) Waggoner, R. A.; Blum, F. D.; Lang, J. C. *Macromolecules* **1995**, *28*, 2658.
- (27) Hansen, P. L.; Cohen, J. A.; Podgornik, R.; Parsegian, V. A. *Biophys. J.* **2003**, *84*, 350.
- (28) Walder, R.; Nelson, N.; Schwartz, D. K. *Phys. Rev. Lett.* **2011**, *107*, No. 156102.
- (29) Kastantin, M.; Schwartz, D. K. *Microsc. Microanal.* **2012**, *18*, 793.
- (30) Douglas, J. F.; Johnson, H. E.; Granick, S. *Science* **1993**, *262*, 2010.
- (31) Honciuc, A.; Schwartz, D. K. *J. Am. Chem. Soc.* **2009**, *131*, 5973.
- (32) Bychuk, O. V.; O'Shaughnessy, B. *Phys. Rev. Lett.* **1995**, *74*, 1795.
- (33) Bychuk, O. V.; O'Shaughnessy, B. *J. Phys. II* **1994**, *4*, 1135.
- (34) Klafter, J.; Shlesinger, M. F. *Proc. Natl. Acad. Sci. U.S.A.* **1986**, *83*, 848.
- (35) Xu, Q.; Feng, L.; Sha, R.; Seeman, N. C.; Chaikin, P. M. *Phys. Rev. Lett.* **2011**, *106*, No. 228102.
- (36) O'Shaughnessy, B.; Vavylonis, D. *Eur. Phys. J. E* **2003**, *11*, 213.
- (37) Frantz, P.; Granick, S. *Phys. Rev. Lett.* **1991**, *66*, 899.
- (38) Wang, Y.; Rajagopalan, R.; Mattice, W. L. *Phys. Rev. Lett.* **1995**, *74*, 2503.
- (39) Cohen Stuart, M. A.; Cosgrove, T.; Vincent, B. *Adv. Colloid Interface Sci.* **1985**, *24*, 143.
- (40) Stuart, M. C.; Waajen, F. H.; Cosgrove, T.; Vincent, B.; Crowley, T. L. *Macromolecules* **1984**, *17*, 1825.